



**A Spatial Ecosystem And Populations Dynamics Model
(SEAPODYM) for tuna and associated oceanic top-predator
species: Part II – Tuna populations and fisheries**

Patrick Lehodey

Oceanic Fisheries Programme
Secretariat of the Pacific Community
Noumea, New Caledonia

July 2004

A Spatial Ecosystem And Populations Dynamics Model (SEAPODYM) for
tuna and associated oceanic top-predator species:
Part II - Tuna populations and fisheries

Introduction

Fishes dominate the upper trophic levels of the pelagic ecosystem, although these groups also include large-size cephalopods, sea turtles, marine mammals and sea birds. Most of the information on the composition of these groups is due to the fisheries, because these fish are either target species or by-catch species.

Skipjack tuna (*Katsuwonus pelamis*) is the most abundant and productive species in the tropical Pacific and constitutes the fourth largest fishery in the world (FAO 2002; ~1.9 million t yr⁻¹). A large part of this skipjack catch (> 1million t) comes from the warm waters of the western and central Pacific Ocean (WCPO), but warm currents of the Kuroshio and east-Australia extend their distribution to 40°N and 40°S (roughly delineated by the 20°C surface isotherm). With skipjack, tuna surface fisheries (purse seine, pole and line and several various fishing gears) are exploiting yellowfin tuna (*Thunnus albacares*) that provided ~ 520,000 t year⁻¹ in average for the period 1995-2002 (~380,000 t in the WCPO and ~140,000 t in the EPO), to which it should be added ~68,000 t of large adult fish that are caught by the longline fishery. Skipjack and yellowfin tuna are fast growing, especially in their first year of life. Skipjack has a relatively short lifespan (4-5 years for most of the individuals). The longest period at liberty for a recaptured yellowfin, tagged in the western Pacific at about 1 year of age, is currently 6 years. Skipjack and yellowfin tuna have early age at first maturity (9-10 mo and 12-15 mo for skipjack and yellowfin respectively), year-round spawning and high fecundity, and relatively high natural mortality rate. Juveniles of other tropical tuna, particularly bigeye tuna (*Thunnus obesus*) are frequently found together with skipjack and yellowfin tuna in the surface layer, especially around drifting logs that aggregate many epipelagic species.

With these well-known species, there are many other scombrids (*Auxis sp.*, *Euthynnus spp.*, *Sarda spp.*, *Scomberomorus spp.*, *Scomber spp.*, etc...), and a large diversity of piscivorous fish (Gempylidae, Carangidae, Coryphaenidae, Trichiuridae, Alepisauridae, etc...) and juveniles of larger predators (sharks, marlins, swordfish and sailfish). Most of these species are typically predators of the epipelagic micronekton but many of them are taking advantage of the vertical migration of meso- and bathypelagic species that are more particularly vulnerable in the upper layer during sunset and sunrise periods. The largest predators of the tropical pelagic foodweb include adult tuna (*Thunnus albacares*, *Thunnus obesus*, *Thunnus alalunga*), broadbill swordfish (*Xiphias gladius*), marlin and sailfish: Indo-Pacific blue marlin (*Makaira mazara*), black marlin (*Makaira indica*), striped marlin (*Tetrapturus audax*), Shortbill spearfish (*Tetrapturus angustirostris*) and Indo-Pacific sailfish (*Istiophorus platypterus*), pelagic sharks, seabirds and marine mammals.

As they become older and larger, tuna swim deeper. Adult yellowfin and bigeye tuna are exploited with large adult albacore tuna by the longline fishery throughout the tropical and subtropical oceans. Bigeye tuna reach larger sizes (max. FL ~200 cm) than yellowfin and

have a longer lifespan (>10 years). To varying degrees, all tunas can thermoregulate, using a specialized countercurrent heat exchange system: the 'rete mirabile'. Species with well-developed rete (typically bigeye tuna) have the most extended temperature range and hence a larger latitudinal and vertical temperature habitat. Bigeye tuna are exploring deeper (> 600 m) layer than yellowfin tuna, and skipjack tuna is usually confined to the upper mixed-layer, though able to dive below 200 m occasionally. All tuna species have highly opportunistic feeding behavior resulting in a very large spectrum of prey species from a few millimeters (e.g., euphausiids and amphipods) to several centimeters (shrimps, squids and fish, including their own juveniles) in size. However, it seems that differences in vertical behavior can be also identified through detailed analyses of the prey species, bigeye tuna accessing deeper micro- and macronekton species.

In summary, top predators in the tropical pelagic food web are essentially opportunistic omnivorous predators. Their diets reflect both the faunal assemblage of the component of the ecosystem that they explore and their aptitude to capture prey species at different periods of the day (i.e., daytime, nighttime, twilight hours). It seems that most of them are in the upper layer during the night. But high sensory specialisation (e.g. olfaction in sharks, vision in bigeye tuna, swordfish and cephalopods or echolocation in marine mammals), and morphological and physiological adaptations (e.g., rete mirabile) allow them also to exploit the dark and colder deeper layers.

This document presents an update of the modeling approach used for describing the dynamics of the tuna populations, and potentially other oceanic top-predator species, in the spatial ecosystem model SEAPODYM. As for the intermediate components (see part I), a number of changes have been realized from the first version (SEPODYM). In particular, with the development of several forage components it was necessary to reconsider how the tuna species were linked to these different food sources.

Results from a first application to 2 tuna species (skipjack and yellowfin) are presented and discussed with the future developments and applications that can be envisaged for providing a useful tool for the management of tuna stocks in the context of climate and ecosystem variability, complementarily with statistical population models.

Top-predators (tuna) dynamics Modeling

The modeling approach for the tuna population dynamics has been first described in Bertignac et al. (1998), and modified in Lehodey (2001) and Lehodey et al. (2003). Populations are age-structured and movements described with an advection-diffusion equation. Surface currents passively transport tuna larvae, then, young and adult tuna movements are constrained by the adult habitat index. Diffusion and advection are proportional to the size of the fish (Lehodey et al., 2003) and the advection term is proportional to the gradient of the adult habitat. This latter has been modified to take into account the changes in the modeling of the forage components.

While the adult habitat index constrains the movement, a spawning habitat index (H_s) is used to constrain the recruitment to environmental conditions (Lehodey et al., 2003).

$$H_s = \cdot_s \bullet e^{\alpha \ln \left[\frac{P}{F_0 + \left[\frac{24-DL}{24} F_2 \right]} \right]} \quad (1)$$

with \cdot_s the spawning temperature function following a normal distribution $N(T_s, \sigma_s)$ of standard deviation σ and optimal mean temperature T_s . P is the primary production (a proxy for the abundance of food for larvae), F_0 and F_2 are biomasses of epi- and migrant-pelagic forage used as a proxy for the abundance of predator of larvae. The migrant forage is corrected proportionally to the time spent in the upper layer where are the tuna larvae and juveniles. Thus, four mechanisms control the survival of larvae and the subsequent recruitment: the extension of the spawning temperature habitat, the coincidence of spawning with presence or absence (match/mismatch) of food, but also presence or absence of predators, and the oceanic circulation that can create retention of the larvae in favourable areas or conversely move the larvae in unfavourable zones. The initial number of larvae that survive the first month after spawning and enter in the first cohort is given by the product of a recruitment scaling value (R_s) and the spawning habitat index (this process being continuous in time). R_s is used to scale the total average biomass to independent estimates (i.e. from the MULTIFAN-CL model).

Adult habitat index H_a

To define the adult habitat index, first, an accessibility coefficient (τ_n) is calculated for each forage component n , based on the constraints/affinities of the predator species for the physical conditions that characterize the water layer inhabited by the forage component. Habitat functions for two critical parameters for tuna, temperature (\cdot_a) and dissolved oxygen content (O_a), are considered. The accessibility coefficient is the product of the indices obtained from these two functions (temperature and oxygen) for the layer considered (eq. 2).

$$\tau_n = I_{\cdot_a, n} \cdot I_{O_a, n} \quad (2)$$

In the case of the migrant mesopelagic forage, it is necessary to calculate the mean temperature and oxygen based on the day length DL (eq. 8 in part I). For example, for the temperature, the index used in the accessibility coefficient for this component is:

$$I_{\cdot_a} = \frac{[I_{\cdot_a1} \cdot (24 - DL)] + [I_{\cdot_a2} \cdot DL]}{24} \quad (3)$$

with I_{\cdot_a1} and I_{\cdot_a2} the indices from the temperature function calculated with the temperature in the upper and deep layer respectively.

As in the spawning index, the temperature function follows a normal distribution: $\cdot_a = N(T_a, \sigma_a)$. All tuna species are known to spawn in warm waters (typically above 25-26 °C), while their feeding habitat is covering a larger temperature range. Moreover, as they grow, their optimal temperatures decrease due to the development of the *rete mirabile* and higher accumulation of heat from larger body mass. Consequently, the optimal mean temperature T_a was linearly linked to the age by equation (4):

$$T_a = \frac{(T_{min} - T_s)}{K} \bullet age + T_s \quad (4)$$

where T_{min} is the optimal mean temperature of the oldest cohort in the species population (Figure 1) and K the total number of cohorts of the species.

For the oxygen, a sigmoid function is used since only minimum values constrain the accessibility to the water layer associated to the forage component. The habitat index value for n forage (F) components is then:

$$H_a = \sum \left[\tau_n \frac{F_n}{F_{max,n}} \right] \quad (5)$$

$F_{max,n}$ being used for standardizing F between 0 and 1.

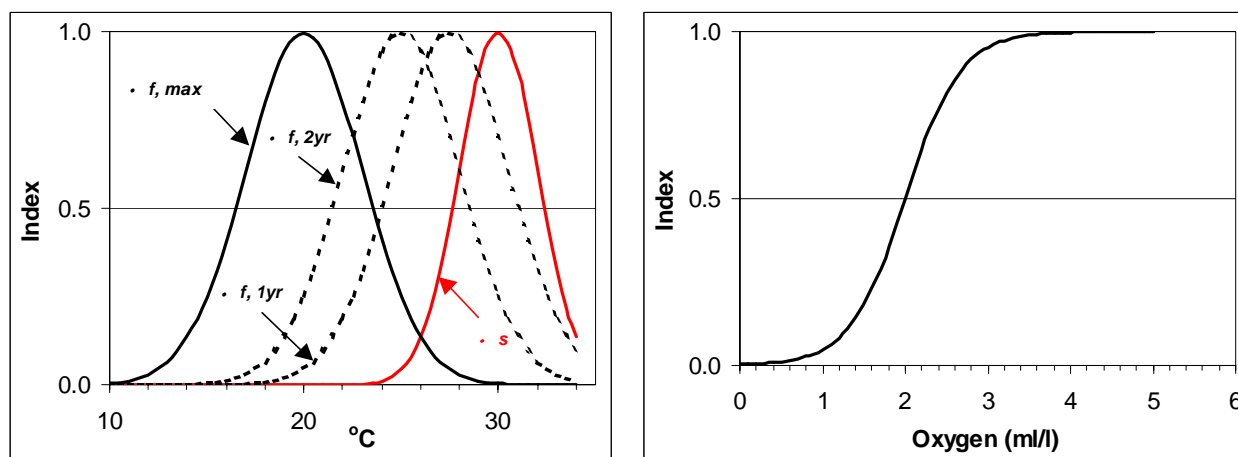


Figure 1. Left: change in temperature function with age from age 0 (spawning) to maximum age; right: habitat function for the oxygen.

Spawning seasonality

Typical tropical tuna species like skipjack and yellowfin are thought to spawn opportunistically in warm waters, and do not show clear spawning seasonality. With increasing affinities for colder waters and longer life span, in relation also with the extension of the feeding habitat to the temperate regions, tuna species appear to develop such seasonality, lightly marked for bigeye, more evident for albacore and fully obvious for the temperate bluefin tuna. Also, with the increasing seasonal effect, the spawning grounds seem becoming more limited in space (and time by definition). This is a good illustration of an evolutionary history between r- and K- strategies. In an r-situation, organisms invest in quick reproduction, in a K-situation they will rather invest in prolonged development and long life. Usually r-selection correspond to an adaptation to a risky environment and K-selection to a more predictable (sure) environment. While seasonality is the strongest and “predictable” climate variability that affect bluefin tuna in temperate regions, it is the interannual and less predictable ENSO signal that controls the environmental variability in the western and central

equatorial regions that is the core habitat of skipjack tuna. The seasonal cycle of reproduction and its associated maturation process can be easily believed under the control of strong seasonal factors, e.g. changes in temperature and light (day length), while the seasonal spawning grounds result from natural selection and evolution in the species life history under the constrain of environmental variability.

Trying to reproduce the increasing seasonal effect on tuna species with colder temperature affinities, a seasonal effect is included, based on the following assumptions:

- (i) With the seasonal spawning period becoming closer in time, adult tuna tend to direct their movements to find a place with the same environmental conditions than those occurring during their birth (Cury, 1994).
- (ii) These conditions are defined by the spawning habitat index H_s .
- (iii) The seasonal effect is controlled by the cycle of day length (both in time and intensity, i.e. increasing with latitude).
- (iv) The triggering effect for gradually switching from the feeding habitat to the spawning habitat is the increasing day of length (positive gradient)

Thus, using a function based on the day length, it is easy to change the directed movement according to either the feeding or the spawning habitat index. This switch would have limited impact in the equatorial region because of warm temperature close to those of the spawning habitat and because of the limited range of change in the day length. For opposite reasons, the behaviour of (mature) tuna could change drastically in the subtropical and temperate regions. In a first hypothesis, mature fish are supposed to move toward their spawning grounds when the day length is increasing. First, the gradient of day length (G_d) is calculated and standardised between -1 and 1 (Figure 2) based on the maximum value obtained for the highest potential latitude of their habitat (60°N). Then eq. (4) and (5) are changed to eq. (6) and (7) respectively to consider feeding and spawning effects varying with the positive gradient of day length, given the latitude and the day of the year.

$$T_a = T_{age} + G_d \bullet (T_s - T_{age}) \quad (6)$$

with T_{age} the optimal temperature for a given age defined by eq. (4).

$$H_a = \sum \left[\tau_n \bullet \frac{F_n}{F_{\max, n}} \right] \bullet e^{(\alpha G_d) \ln \left[\frac{P}{\left(F_0 + \left[\frac{24 - DL}{24} F_2 \right] \right)} \right]} \quad (7)$$

It is also worth noting that as tuna species develop a stronger seasonal spawning pattern, limiting the spawning in time and space, this likely makes the recruitment more sensitive to the spawning biomass. Such impacts on the tuna population can be investigated by changing eq. (1) to integrate a spatially explicit stock-recruitment relationship in multiplying the previous index by a measure of the effect of spawning (ie, adult) biomass B_s in each cell of the grid. For example:

$$H_s = \Downarrow \log[B_s] \cdot s e^{[\alpha \text{Ln}(P/F)]} \quad (8)$$

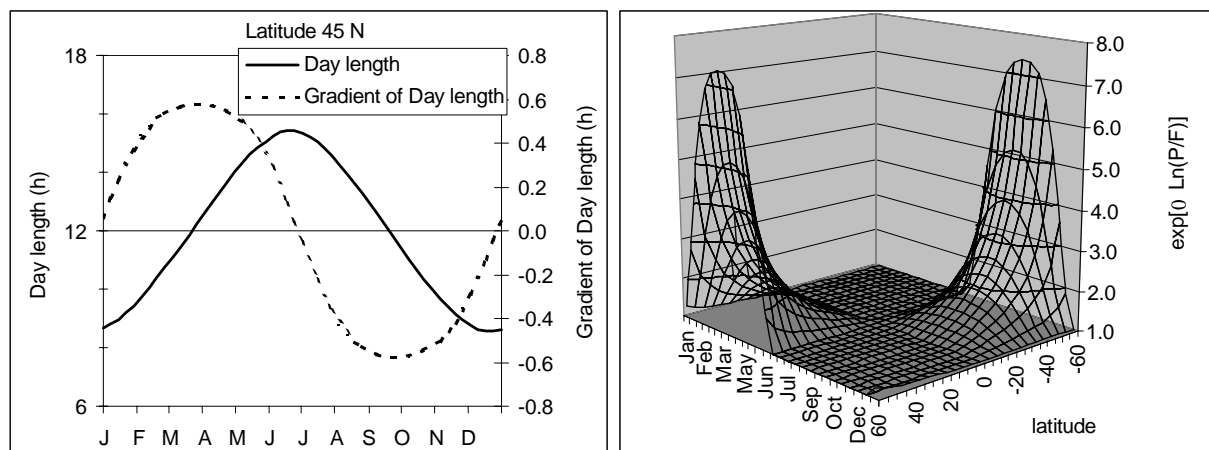


Figure 2. Examples of (left) seasonal cycle of day length at 45°N, with gradient of day length standardised between -1 and 1 using the maximal value at 60°N, and (right) change in the exponential term of H_a (with $\alpha=1$ and $P/F=2$) according to equation (7).

Prey-predators coupling

Given that there are several forage components, it is necessary to revise the approach used for coupling the forage mortality to the density of predators that was initially described in Lehodey (2001). In the previous version, the forage mortality was linked to the tuna density by applying first a specific local mortality μ_n resulting from the food requirements of tuna population described in the model, then a mean residual mortality μ_r which is the difference between the total mortality μ and the mean specific mortality μ_n over the area occupied by tuna. Therefore, the total forage biomass over the whole area remains equal to the total forage biomass calculated in the case of a constant μ_r , but the spatial distribution linking the density of tuna may be different (see previous reference). This approach is useful as it is possible to have from zero to all potential predators species explicitly described in the model. As a counterpart, this is based on the assumption that the predators present an ‘ideal free distribution’, such that the total forage mortality by these species would be the same everywhere and equal to μ_r . This assumption does not appear unrealistic when considering both the horizontal and vertical distribution of the main tuna species together with those of other large oceanic predators.

It is possible to use the same approach with several forage components, at the condition of defining for each predator species the forage required from each component. This is done using the accessibility coefficient τ_n defined in eq. (2). The ratio of forage of a given component that contributes to the total food ration is:

$$\mu_n = \frac{\tau_n}{\sum \tau_n} \quad (9)$$

then, the forage required from the component n by the tuna species (F_{Rn}) is calculated by knowing a daily food ration r relative to its weight-at-age w and the ratio μ_n obtained from eq. (9). The specific mortality rate is defined as the ratio of the forage biomass requirement (F_{Rn}) for the species to the forage biomass available F_n (eq. 11):

$$F_{Rn} = \sum_{age,i,j} (N_{age,i,j} \cdot w_{age} \cdot r_{age} \cdot n_{age}) \quad (10)$$

and the local specific mortality n on the forage component n is the ratio between the forage required and the forage available, calculated for each age class in each cell of indices i and j .

The mean specific mortality over the whole area occupied by the predator species is:

$$\bar{n} = \frac{\sum F_{Rn}}{\sum F_n} \quad (11)$$

Natural and fishing mortality

The total mortality rate (Z) is the sum of natural (M) and fishing mortality (f). Natural mortality can be described as the sum of two main causes. The mortality occurring during the juvenile and young phases (M_p) that is mainly due to starvation and predation, and the natural mortality associated to senescence and diseases in the adult phase (M_s). These two sources are represented by equations 12 and 13, the sum of which gives the average natural mortality-at-age, and illustrated on the figure 3 for skipjack, yellowfin and bigeye tuna. The parameterization is defined to obtain coefficients of natural mortality-at-age in agreement with those estimated statistically with MULTIFAN-CL and to have coherent parameters between species (Table 1). For example, trends in natural mortality in early life stages are expected similar, although absolute values can decrease from skipjack to yellowfin and from yellowfin to bigeye in respect with their increasing life span associated to a more developed K- strategy (i.e., selection of better spawning time and spawning ground allowing a lower larvae mortality).

$$\bar{M}_{p_{age}} = M_{p_{max}} \cdot e^{(-c_1 \cdot age)} \quad (12)$$

$$\bar{M}_{s_{age}} = \frac{M_{s_{max}}}{1 + e^{(c_2 \cdot (age - c_3))}} \quad (13)$$

In addition, the total natural mortality values obtained from eq. (12) and (13) are expressed in terms of the habitat (eq. 14) assuming that the mortality rates are increasing in unfavourable habitat. The parameterization has been defined to exponentially increase the mortality rates when habitat values are below 0.1. The habitat index used is the spawning habitat for the first age class and the adult habitat for the other age classes.

$$M_{age} = 1 - \frac{(1 - \bar{M}_{age}) \cdot H_{age}}{(c_4 + H_{age})} \quad (14)$$

The fishing mortality is proportional to the fishing effort, the catchability coefficient of the fishery and the selectivity coefficient for the gear and age (size) considered.

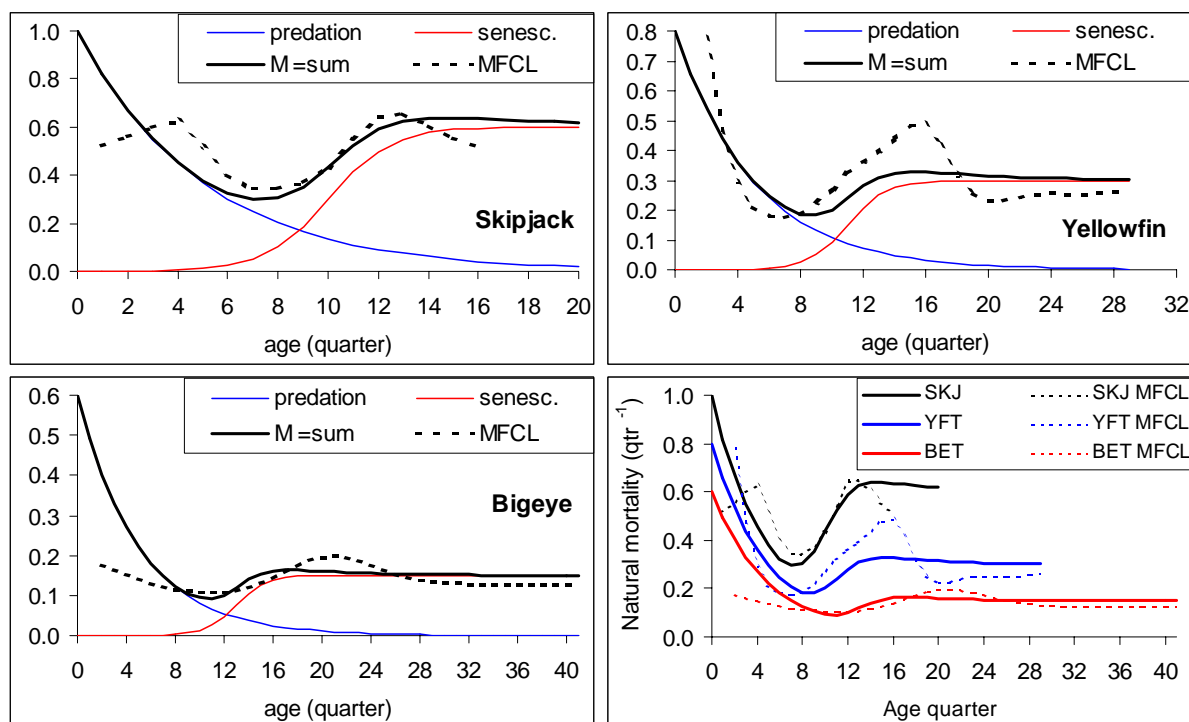


Figure 3. Natural mortality of skipjack, yellowfin and bigeye tuna species defined in the model (thick curves) and compared to estimates from MULTIFAN-CL (dotted curves).

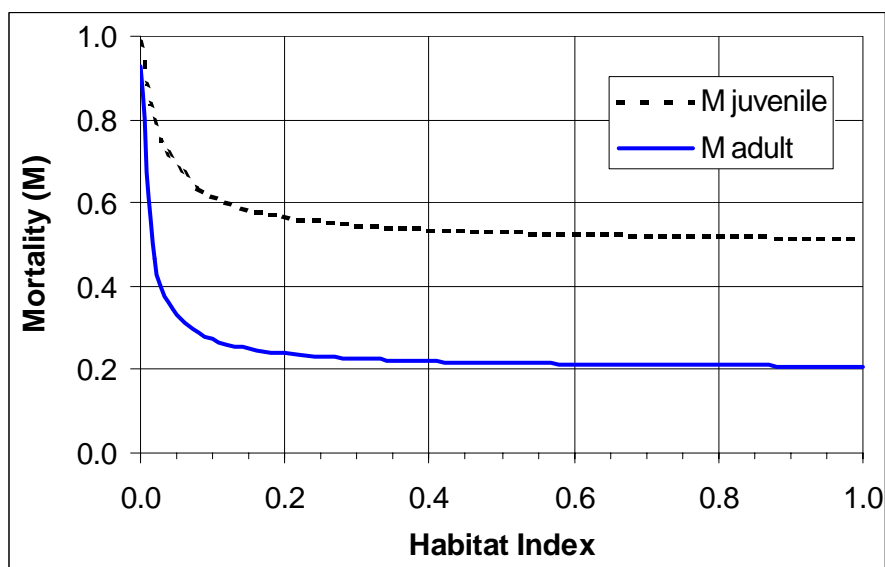


Figure 4. Functions based on equation 14 to represent the increase in natural mortality due to very low values of Habitat index. Examples are presented for a mean natural mortality of 0.2 and 0.5, and coefficient c_4 of 0.01 and 0.03, for adult and juvenile respectively.

Table 1. Parameterization of the natural mortality functions for skipjack, yellowfin and bigeye tuna species

	Skipjack	yellowfin	bigeye
M_{pmax} (qtr ⁻¹)	1	0.8	0.6
M_{smax} (qtr ⁻¹)	0.6	0.3	0.15
c_1	0.2	0.2	0.2
c_2	-0.8	-0.8	-0.8
c_3 (qtr)	10	11	13

Application to two tuna populations

The parameterisation for each tuna species was estimated using single species, multiple-fisheries simulations (cf annexes). The spatial resolution is one degree square and the time step is 30 d. The physical-biogeochemical environmental predicted fields are those of the 1948-2002 ESSIC run used in part I for the forage simulations. Monthly climatologies of these variables are used in the initialization to build up the population during a time period longer than the maximum age of the species that has the longer life span. It is possible to use the same climatology for extending the simulation at the end or after any given year of the real time simulation to provide a forecast over a few following years based on these mean environmental distributions.

Definition of Fisheries

A simple definition of tuna fisheries was sought to keep a reasonable number of fisheries in a multi-species simulation. The first criteria was the fishing gear, but it is also necessary to consider some large spatial-scale stratification, different fishing strategies, and also changes in the longline gear associated to a shift in the fishing strategy for fishing deeper and targeting bigeye tuna (Table 2). Each fishery has one constant catchability coefficient and an age-based selectivity function. The selectivity functions are adjusted to obtain predicted length frequency distributions of catch in agreement with the observed distribution. Fishing effort of each fleet varies by month and in space at a monthly one-degree square resolution. When the fishing data were at a lower resolution (e.g., longline fishing data are at a 5-degree square resolution), the fishing effort was subdivided accordingly. The catchability coefficients are scaled to obtain estimated catches at the same average level as observed catches. Results of the simulation are evaluated by comparing observed and predicted total monthly catch, spatial distribution of catch and distribution of catch length frequencies for each fishery (cf annexes).

Table 2: Definition of fisheries used in the single and multi-species simulations

	code	Fishery	Fleets Nationality / sources
1	PLJAP	Japanese Pole and line North of 25N	Japan
2	PLTRO	All tropical (South of 25N) Pole and line	Japan, Solomon, Fiji...
3	PSEANI	EPO Purse seine sets associated with animals	IATTC
4	PSEFAD	EPO Purse seine sets associated with FAD	IATTC
5	PSELOG	EPO Purse seine sets associated with LOG	IATTC
6	PSEUNA	EPO Purse seine sets unassociated	IATTC
7	PSWDIV	WCPO Purse seine sets associated with Animal or unknown	All WCPO fleets, except domestic Philippines and Indonesia
8	PSWFAD	WCPO Purse seine sets associated with FAD	All WCPO fleets, except domestic Philippines and Indonesia
9	PSWLOG	WCPO Purse seine sets associated with LOG	All WCPO fleets, except domestic Philippines and Indonesia
10	PSWUNA	WCPO Purse seine sets unassociated	All WCPO fleets, except domestic Philippines and Indonesia
11	LLP80	All longlines before 1980 (= shallow)	Japan, China, Taiwan ROC
12	LLDEEP	All deep longline after 1980	Japan, FSM, New Caledonia, French Polynesia, New Zealand, Fiji, Tonga, Cooks
13	LLSHW	All shallow longline after 1980	China, Taiwan ROC
14	LLMIX	Mixed longline sets after 1980	Australia
15	LLUNKN	Unknown sets after 1980	The remainder of the fleets
16	GI	Gillnet	JP and TW
17	TR	Troll	NZ and US troll

Results

Single species simulation results are presented in annexes I and II for skipjack and yellowfin respectively. They are preliminary results, as the changes in the structure of the model require many more simulations for adjusting and testing the sensitivity of the parameters. In particular, catchability coefficient for yellowfin fisheries are not all yet adequately defined (cf CPUE indices in annex II). One simulation takes between 7 (skipjack) and 10 hours (yellowfin) on a PC Pentium 4 2.5Ghz.

Once the different age structures and natural mortality coefficients are defined for each species, there are finally relatively limited differences between species for the parameterisation of the habitat and movement. Optimal temperature values were shifted from

29 to 28°C for the spawning habitat and from 25 to 22°C for the feeding habitat of skipjack and yellowfin respectively. Values of the movement coefficients are the same, but as the final movement is linked to the size of the fish, adult yellowfin can move faster than adult skipjack.

Integrating these few differences of habitat definition into different spatio-temporal population dynamics produces complex and different results with potential positive or negative feedback mechanisms. For example, the lower optimal temperature value for yellowfin increases its horizontal and vertical habitat relatively to skipjack. Therefore, adult yellowfin have more capability to move toward regions where forage density is higher (and temperature lower), e.g., in the eastern Pacific, and to increase the percentage of deep forage in their diet, although it seems not too different from skipjack in average (Figure 5). While their density increases, they increase the mortality on the forage, and since the P/F ratio increases, the spawning habitat increases. This mechanism creates a positive feedback: the adults eat the predators of their eggs. However when the forage mortality is too high, adult habitat decreases and the fish leave the zone. Sensitivity of the model to these mechanisms needs to be evaluated.

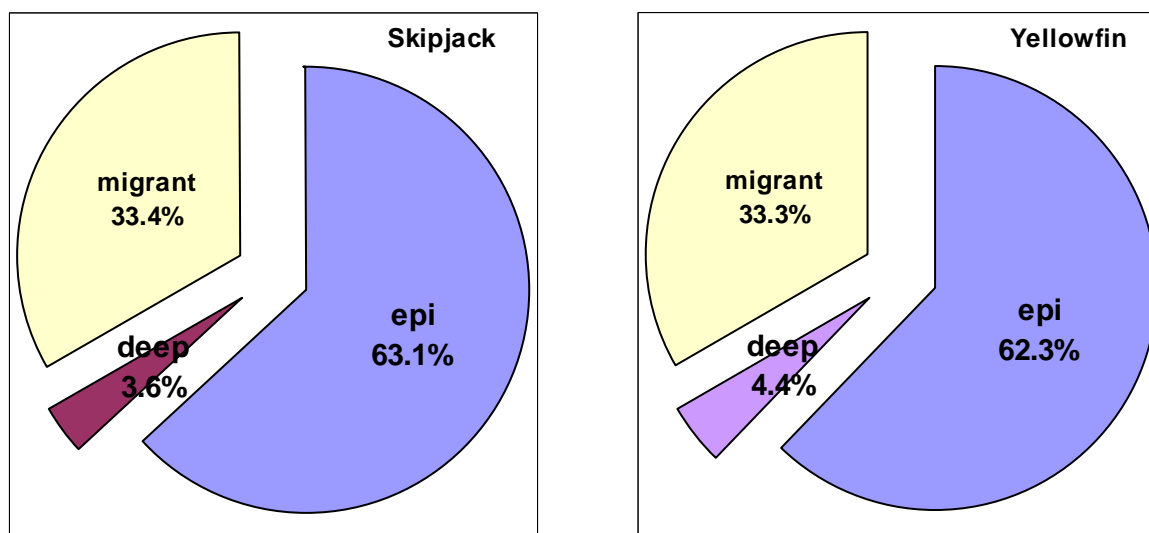


Figure 5. Average percentages of forage consumed by skipjack and yellowfin based on their accessibility to each component of forage

Simulations were evaluated by comparing predictions and observations. First, selectivity coefficients of the fisheries were defined to have an agreement between predicted and observed length frequencies of the catch (see annexes, sections 2). Predicted catch length frequencies are reasonably well reproduced although it is not possible to represent the portion of the largest individuals. This is because the growth is simply defined by constant size-at-age coefficient with a L_s lower than the maximum size observed. This could be improved by increasing the value of L_s , or more interestingly by introducing variability in the growth linked to the environmental parameters (temperature, food).

The bimodal distribution in the yellowfin length frequency distribution of catch from the unassociated purse seine fishery in the western Pacific is not reproduced. This bimodal distribution could be due to non-predicted movements of adults or/and to change in

catchability. Previous analyses (Lehodey 2000) have shown that CPUE of purse seiners in the western Pacific are strongly affected by ENSO related changes in the depth of the thermocline, the catchability of adult yellowfin increasing during El Niño events in the western Pacific as the thermocline arises. It would be therefore interesting to test if a relationship linking catchability and thermocline depth can reproduce this sort of distribution.

Preliminary tests on the effect of the seasonal function in the definition of the habitat suggests a clear enhancement in the correlation between predicted and observed spatial catch in all the fisheries. But more detailed analyses are needed to investigate how this seasonality affects the movement of fish.

Recruitment and biomass time series estimates were compared with estimates from Multifan-CL for each region used in this statistical model (section 3 in annexes). For skipjack, the fluctuations in the biomass are similar to those predicted in previous simulations with one forage component, though less marked (lower amplitude), likely due to the use of average currents in 0-200m instead of 0-50m, leading to a less dynamic environment. On the other side, the shift leading to a higher productivity regime after the mid-75 appears more clearly. Comparisons between predicted and observed monthly CPUE by fishery (section 4 in annexes) are generally good and monthly spatial correlation between observed and predicted catch oscillate in average between 0.4 and 0.8 for most of the fisheries. There is however an important discrepancy in the skipjack Japanese pole and line, that requires more detailed analyses. But since predicted temperature fields that are used here present a bias in high latitudes (cf part I), this analysis will be conducted after new simulations based on the corrected run.

For yellowfin, the general trend presents limited amplitude in the fluctuation that is more in agreement with the MULTIFAN-CL GLM standardised estimate. The model SEAPODYM does not predict an increase in region 1 as in the statistical estimates and it suggests a large increase in the last year due to the trend in region 2. This trend seems doubtful and could be partly due to incomplete coverage or absence of fishing effort in the last 2 years. More generally, sensitivity in the parameterization needs to be tested to increase the agreement between predicted and observed catch and CPUE.

Discussion

Since its early development in 1995, this model is now entering in a mature phase and is producing promising results for investigating the dynamics of tuna populations in relation with their pelagic ecosystem and its climate-related variability. However, the numerous changes introduced in the structure of the model require now running a large number of simulations to test the sensitivity of the parameters and to obtain the best possible agreement between observations and predictions.

The model is particularly helpful in investigating the recruitment mechanisms. Results from statistical population dynamics modelling point to a clear link between tuna recruitment and climatic fluctuations (Lehodey et al 2003). They also indicate that not all tuna respond in the same way to ENSO cycles. Recruitment of tropical tunas (such as skipjack and yellowfin) increased following El Niño events. Subtropical tunas (i.e. south Pacific albacore) show the opposite pattern, with low recruitment after El Niño events and high recruitment after La Niña events. SEAPODYM simulations reproduced skipjack recruitment increases in both the

central and western Pacific during El Niño events, a result of four mechanisms: the extension of warm water farther east (ideal spawning habitat is found in warm, 26-30° C water), enhanced food for tuna larvae (due to higher primary production in the west), lower predation of tuna larvae, and retention of the larvae in these favourable areas as a result of ocean currents. The situation is reversed during La Niña events, when westward movement of cold waters reduces spawning success in the central Pacific; then the bulk of recruitment is centred in the warm waters of the western Pacific. Results are more preliminary for yellowfin, but similar mechanisms likely occur for this species and peaks of recruitment are predicted after each major El Niño event.

Several aspects could be still explored and tested with more details in the model: the variability in growth, in natural mortality, and in catchability, e.g. with the depth of the thermocline. There are also several avenues for future improvements and validations.

Introducing the other tuna species (bigeye, albacore) in the model is the first task and will increase confidence in the model if it can reproduce converging results with the statistical estimates, and especially if it can reproduce the opposite fluctuations in the recruitment observed between yellowfin and albacore with the same recruitment mechanisms (previous simulations based on one forage component suggested that this is the case).

When parameterization will be defined for these 4 species, multi-species simulations will be used to investigate if there are strong competition for forage between species and if this affects the spatial distribution and the recruitment of the species.

The implementation of an optimization function for a statistical estimation of the parameters should be also a priority. Though the spatial approach makes this development a difficult task, it is worth to note that this model is strongly constrained by the environment and the mathematical description of the relationships between tuna and this environment. Consequently, there are a limited number of parameters that would need to be considered in the optimization process.

Another way to improve the parameterization is to evaluate the simulation against other modelling approaches. It is done routinely against biomass estimates from statistical models, but comparisons with movement simulations from individual-based models could help also to evaluate the parameterisation of movements. Therefore, behaviour of tuna or other large pelagics predicted with IBMs in the same predicted oceanic environment used/produced by SEAPODYM could be compared to observed movements of individuals marked with electronic tags in selected study areas (cf. Kirby et al., 2004), and to spatial patterns generated at the population level by SEAPODYM (see Fig. 16 in part I). This type of analyses is the objective of the project “Mixed-resolution models for investigating individual to population spatial dynamics of large pelagics” developed between OFP and the PFRP at the University of Hawaii in collaboration with the University of Maryland. It requires increasing spatial and temporal resolution to reproduce at least meso-scale features.

In parallel with the improvement of the model, several fields of applications can be explored already.

Confirmation of multi-decadal regimes of productivity in tuna populations as suggested by both statistical and the present environmental-based estimates are an outstanding issue for tuna fisheries management. They would result of the dominance of either El Niño or La Niña events during decadal periods that create accumulation over time of positive or negative annual recruitments in the populations. Hence, the high frequency ENSO-related recruitment signal is converted into low frequency decadal fluctuations of the population biomass. While it is possible to discriminate two different regimes in tuna recruitment statistical estimates prior and after the mid-1970s, it is too soon to assert that a new decadal regime is affecting tuna stocks in the Pacific Ocean since 1998. On the other hand, the regime shift associated to the PDO in the mid-1940s took place just before the development of the industrial tuna fisheries in the 1950s, and there is consequently insufficient information to know if a shift occurred in tuna stocks with reversed trends to those observed in the mid 1970s (i.e., we would expect an increase in albacore and a decrease in yellowfin and skipjack stocks). Nevertheless, a few indications exist. Despite a limited fishing effort in the early 1950's, the catch rates of yellowfin in longline fisheries declined rapidly. Concerning albacore, catch rates continuously increased during all the 1950s and started decreasing in the 1960s, mainly because of changes in species targeting. Therefore, while it is important to identify in the coming few years if the ecosystem has entered a new regime since 1998, it is also needed to extend and improve our knowledge in a potentially similar shift after 1947. One important source of fishing data that would be useful to rescue concern the Japanese skipjack fisheries. This objective has been included in a new project supported by the OFP and the PFRP (Kirby et al. 2004).

Once the parameterization for a species is defined in SEAPODYM and the simulations validated against observations (fishing data) for the last 50 years of exploitation, it will be possible to run hindcast simulations based on the environmental conditions existing in the periods before the development of industrial fisheries. Similarly, forecast simulations can be produced. At a time scale of a few years, it is possible to use the inertia of the biological signal (i.e., a high/low rate of larvae survival will affect the adult population a few months/years later) to provide the trend in the population. This is implemented in the model already using a climatology (monthly average) of environmental conditions. It is possible to test the predictive skills of this approach by a retrospective analysis. In the future we could also expect to use ENSO forecast for better prediction. At time scales of a few decades, the model would be useful to test different management and economical scenarios, and finally impacts of climate changes under global warming scenario could be explored at the scale of the century.

The spatial aspect of the model and the multi-species multi-fisheries approach present additional interests for management issues. The model can be used to test interactions between fisheries and the impacts of management options on the different species. Biomass of tuna can be calculated by EEZ for discussions at National level, and conservation measures can be tested. For example, the potential impacts and relevance of Marine Reserve Areas on tuna stocks and fisheries can be explored to identify pelagic areas in the open ocean that are key zones (if there are) for ensuring resilience of tuna species and the sustainability of their fisheries. A preliminary study on this subject is supported by the French 'Secrétariat Permanent pour le Pacifique' to consider the following questions:

Given current exploitation rates, stock assessment results and understanding of temporal and spatial variability of stocks, for which tuna species, if any, is the identification of candidate marine reserves recommended?

If so, where should candidate marine reserves be located, taking into account the specificities of the fisheries (location, level of fishing effort/catch, fleet characteristics) and the biological characteristics, life histories and habitat ranges of tunas?

Would optimum candidate marine reserves coincide with high seas enclaves in the Western and Central Pacific and if so, what legal, political and economic implications their designation might have for management?

Or should we consider dynamical marine reserves and if so, what legal, political and economic implications their designation might have for management?

Finally, some important by-catch and associated species (e.g., billfish, blue shark) can be included in the model with the same approach used for tuna or by coupling (online or off-line) SEAPODYM to an IBM model that seems to be more appropriate for some species like marine turtles.

Acknowledgment

This work was supported by the European-funded Pacific Regional Oceanic and Coastal Fisheries Development Programme (PROCFish) of the Oceanic Fisheries Programme of the Secretariat of the Pacific Community.

Reference List

- Bertignac, M., Lehodey, P. and Hampton J., 1998. A spatial population dynamics simulation model of tropical tunas using a habitat index based on environmental parameters. *Fish. Oceanogr.* 7(3/4):326-335.
- Cury P. 1994. Obstinate nature – an ecology of individuals – thoughts on reproductive behaviour and biodiversity. *Can. J. Fish Aquat. Sci.*, 51: 1664-1673
- Hampton J., Kleiber P., Langley A., Hiramatsu K., 2004. Stock assessment of yellowfin tuna in the western and central Pacific Ocean. Oceanic Fisheries Programme, Secretariat of the Pacific Community, Noumea, New Caledonia. 17th SCTB, Majuro. Marshall I., 9-18 Aug 2004. *Working Paper SA-2*:
- Kirby DS, Allain G, Lehodey P, Langley A .2004. Individual/Agent-based modelling of fishes, fishers, and turtles. 17th Meeting of the Standing Committee on Tuna and Billfish, Majuro, Republic of Marshall Islands, 9–18 August 2004, Working Paper ECO–4.
- Kirby DS, Hampton Lehodey P, Langley A Allain V., 2004. Regime Shifts in Western and Central Pacific Ocean Tuna Fisheries. 17th Meeting of the Standing Committee on Tuna and Billfish, Majuro, Republic of Marshall Islands, 9–18 August 2004, Working Paper ECO–5.
- Langley A., Ogura M., Hampton J., 2003. Stock assessment of skipjack tuna in the western and central Pacific Ocean. Oceanic Fisheries Programme, Secretariat of the Pacific Community, Noumea, New Caledonia. 16th SCTB, Mooloolaba, Australia, 9-16 July 2003. Working Paper **SKJ-1**: 43 pp.
- Lehodey P., 2000. Impacts of the El Niño Southern Oscillation on tuna populations and fisheries in the tropical Pacific Ocean. Oceanic Fisheries Programme, Secretariat of the Pacific Community, Noumea, New Caledonia. 13th SCTB, Noumea New Caledonia, 5-12 July 2000. Working Paper RG-1: 32 pp

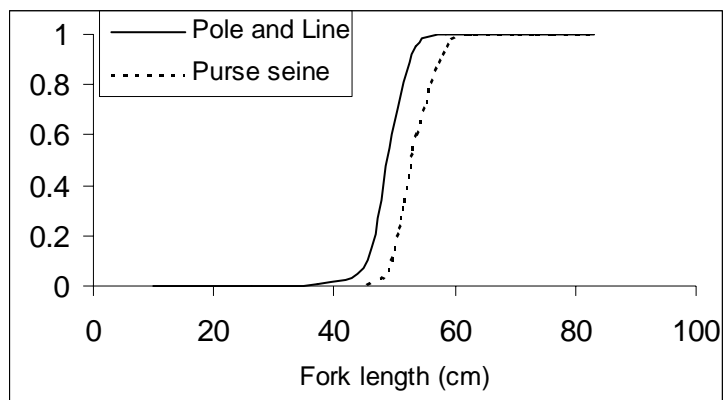
- Lehodey P., Chai F., Hampton J. 2003. Modelling climate-related variability of tuna populations from a coupled ocean-biogeochemical-populations dynamics model. *Fisheries Oceanography*, **12**(4): 483-494
- Lehodey P., 2001. The pelagic ecosystem of the tropical Pacific Ocean: Dynamic spatial modelling and biological consequences of ENSO. *Prog. Oceanogr.* **49**: 439-468.

Annex 1. Single-species simulation for skipjack tuna

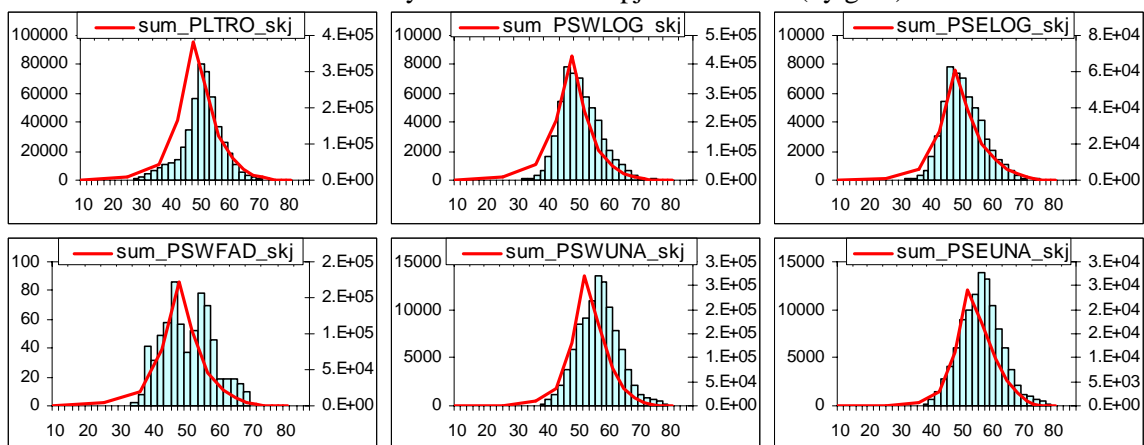
A1-1. Parameterisation

		Unit	Reference
Species code	skj		
Number of age classes	16	Quarter	
Length-at-age	MFCL	Quarter	Hampton (2003)
Weight-at-age	MFCL	Quarter	Hampton (2003)
age of first maturity	3	Quarter	
Larvae-juvenile phase (passive transport)	1	Quarter	
Natural mortality-at-age			
M_{pmax}	1	Quarter ⁻¹	
c_1	0.2		
M_{smax}	0.6	Quarter ⁻¹	
c_2	-0.8		
c_3	10	Quarter	
c_4 juvenile ; adult	0.03; 0.01		
Spawning habitat			
θ (σ_s ; σ_a) based on SST	29; 3	°C	
α	1.4		
Adult feeding habitat			
Temperature θ (σ_s ; σ_a) based on SST for the 0-200m layer and temperature at 200m for the 200-500 m layer	25; 3	°C	
Oxygen S(half value, slope)	2; -0.1	ml .l ⁻¹	
Movement of larvae			
Diffusion	7500	Nm ² .mo ⁻¹	
Advection	Mean currents in upper layer	Nm ² .mo ⁻¹	
Movement of adults			
Diffusion: D_{max}	100,000	Nm ² .mo ⁻¹	
Coeff.: decreasing diffusion with increasing habitat	0.04		
Advection : χ_{max}	30,000	Nm ² .mo ⁻¹	
Coeff.: decreasing advection with increasing habitat	0.4		
Food ration (relative to weight of tuna)	0.05		

A1-2. Selectivity and length frequencies of catch

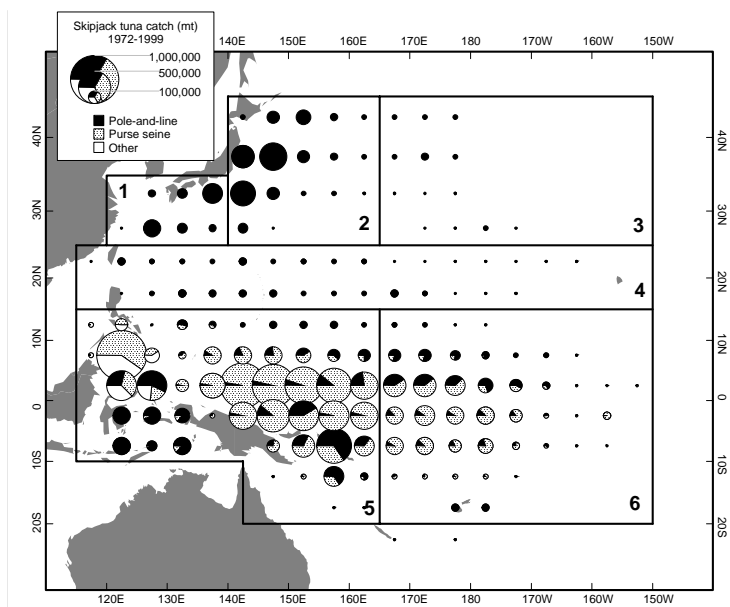


Selectivity curves of the skipjack fisheries (by gear)

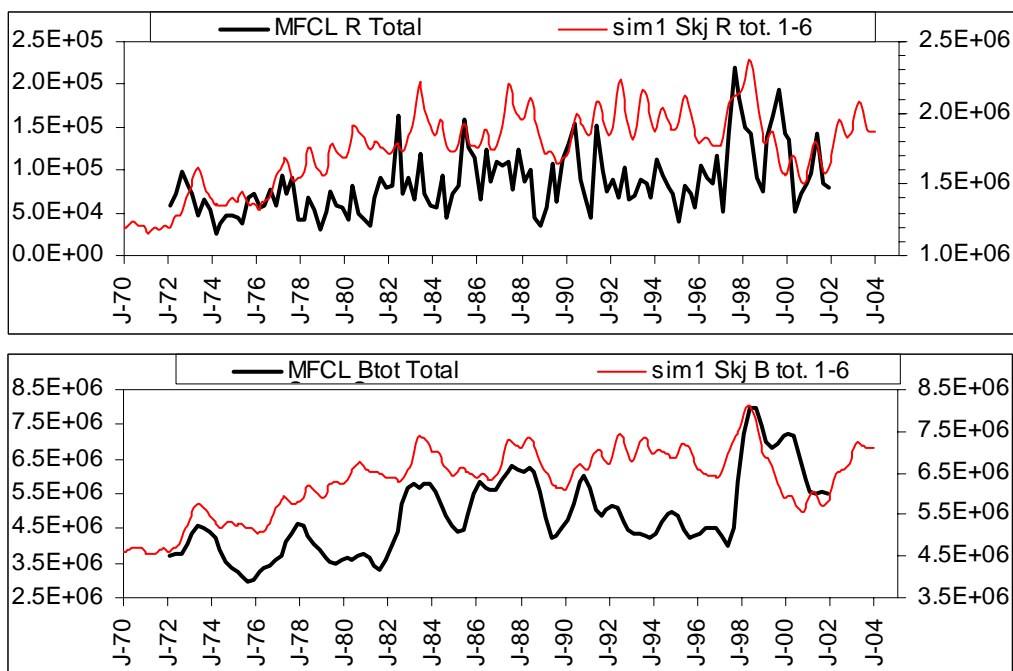


Observed (histograms) and predicted (curves) length frequencies distributions of catch by fishery (see code in Table 2)

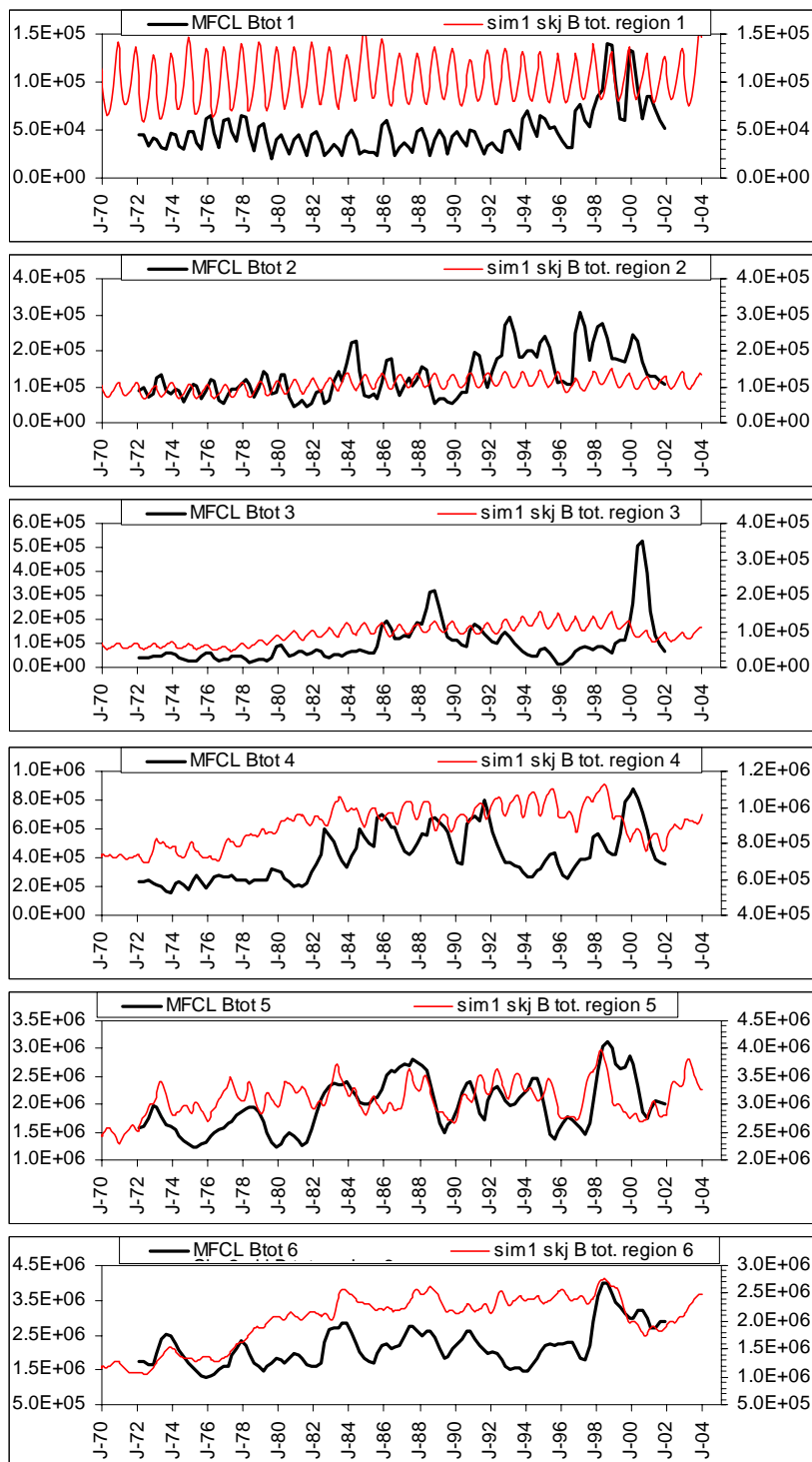
A1-3. Recruitment and biomass



Distribution of total skipjack catches 1972-1999 in relation to the six-region spatial stratification used in the MULTIFAN-CL analysis.

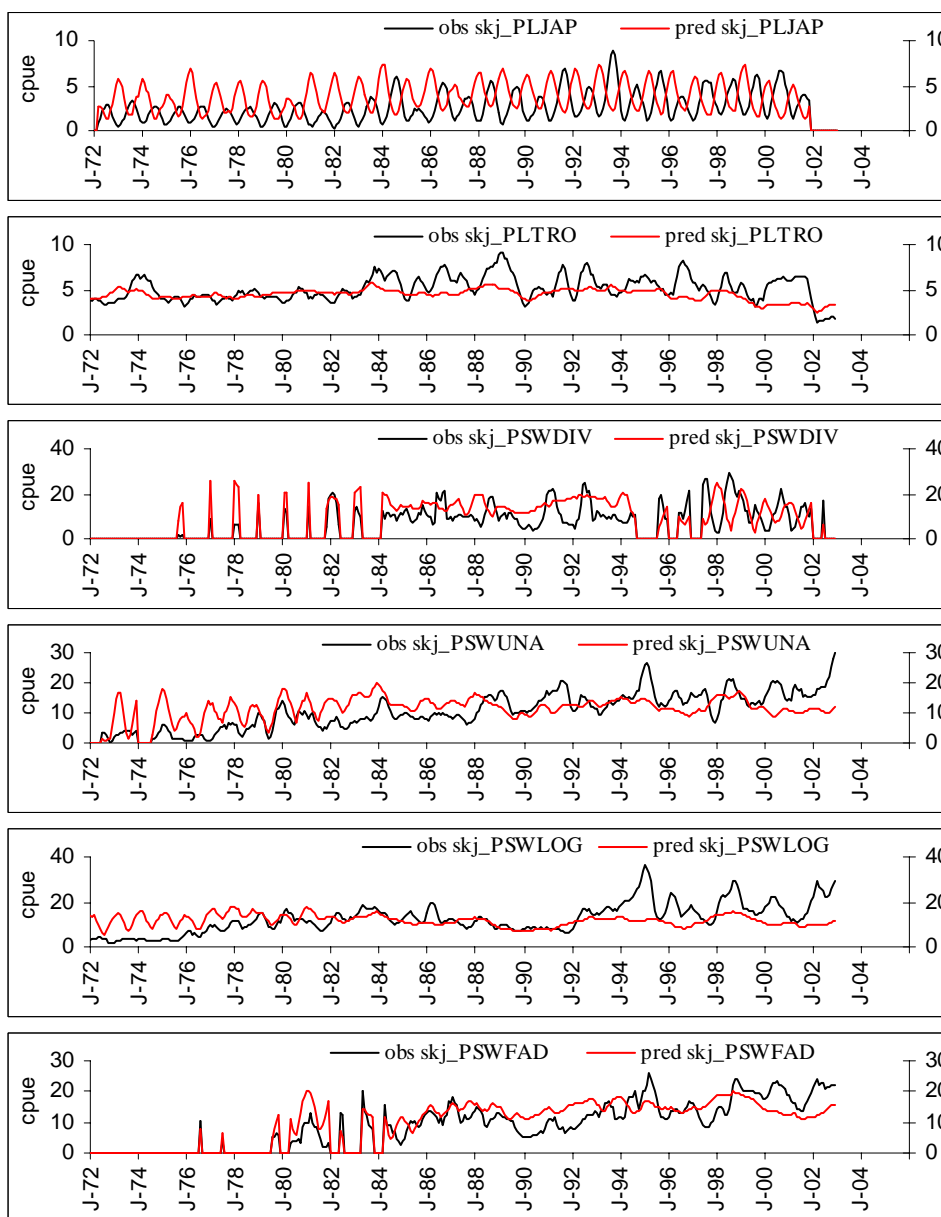


Comparison of skipjack recruitment (top) and total biomass (tonnes) predicted in the WCPO (sum regions 1 to 6) with statistical estimates from MULTIFAN-CL (black curve)

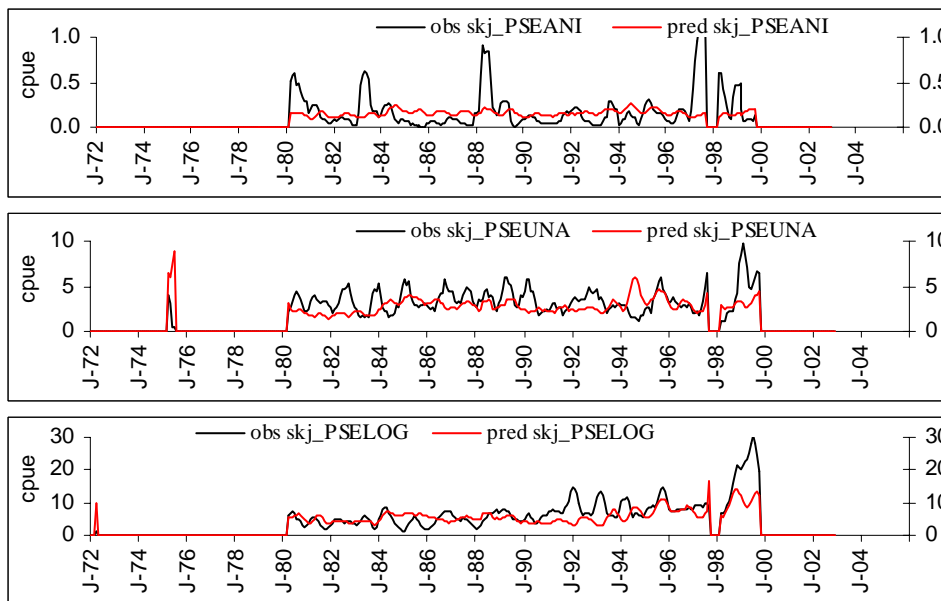


Comparison of total skipjack biomass predicted by region with statistical estimates from MULTIFAN-CL

A1-4. Comparison between predicted and observed CPUE by fishery

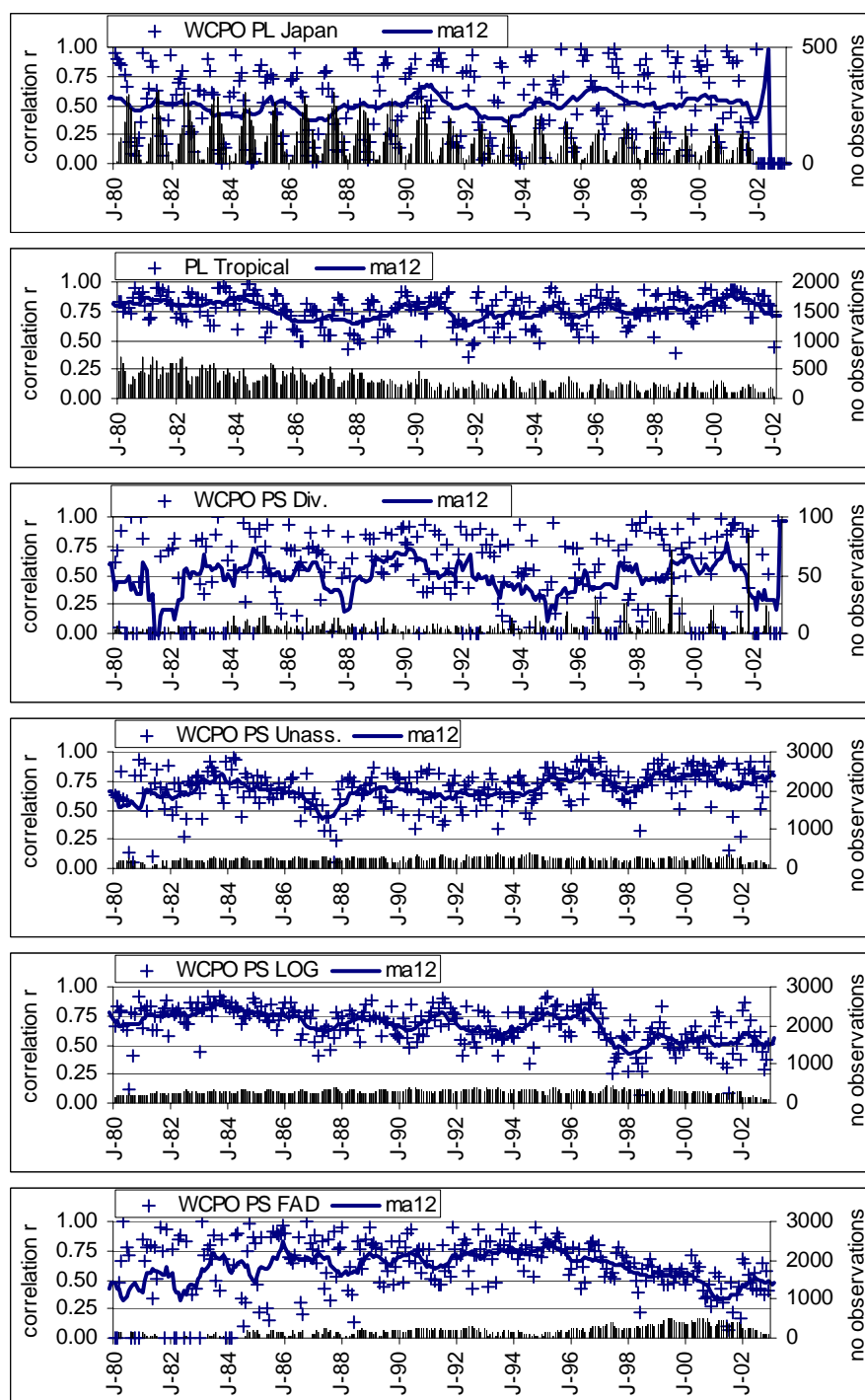


Monthly observed and predicted skipjack CPUE by fishery in the WCPO.

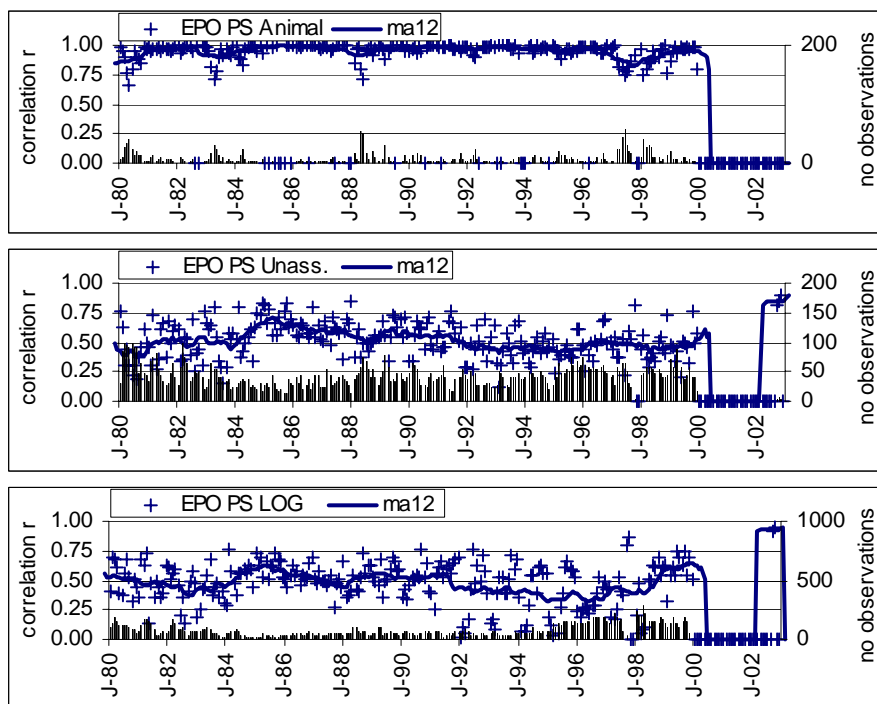


Monthly observed and predicted skipjack CPUE by fishery in the EPO

A1-5. Monthly spatial correlation between observed and predicted catch



Monthly spatial correlation by fishery in the WCPO. Each cross is the r -value of the monthly correlation between 1 degree square spatial predicted and observed catch, the curve is a 12 month moving average and black bars are the number of observations



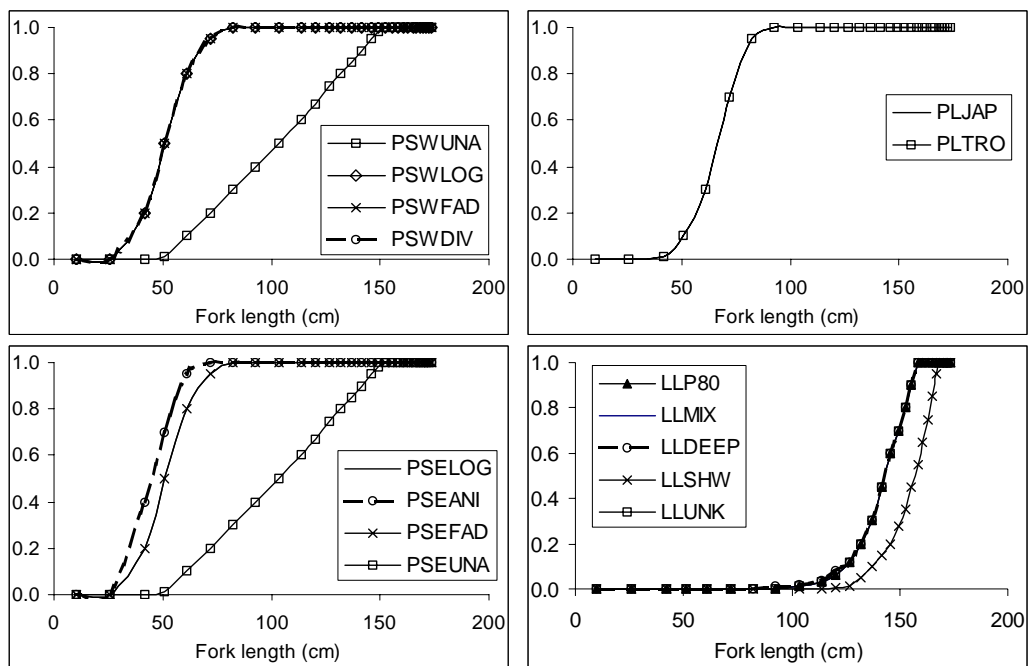
Monthly spatial correlation by fishery in the EPO. Each cross is the r -value of the monthly correlation between 1 degree square spatial predicted and observed catch, the curve is a 12 month moving average and black bars are the number of observations

Annex 2. Single-species simulation for yellowfin tuna

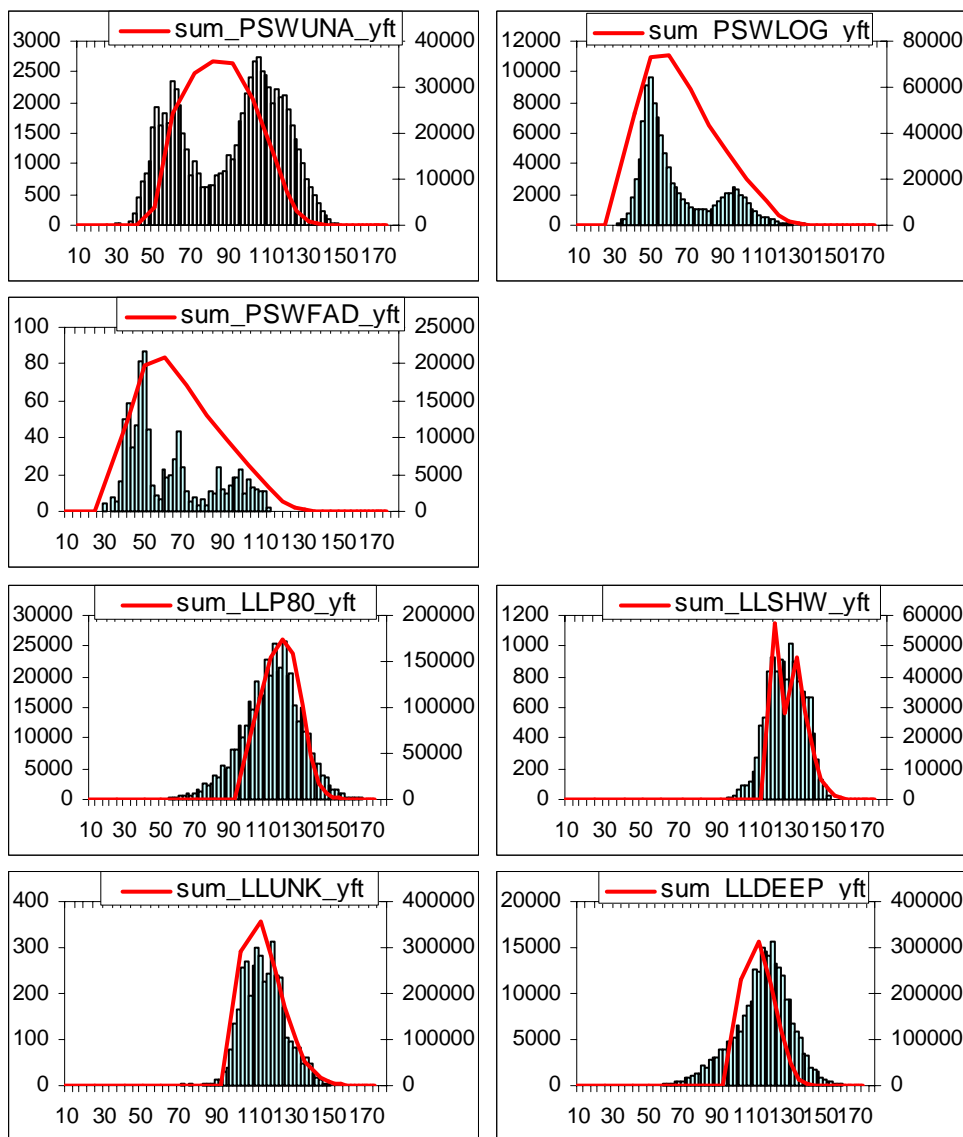
A2-1. Parameterisation

		Unit	Reference
Species code	yft		
Number of age classes	29	Quarter	
Length-at-age	MFCL	Quarter	Hampton et al (2004)
Weight-at-age	MFCL	Quarter	Langley et al (2004)
age of first maturity	6	Quarter	
Larvae-juvenile phase (passive transport)	1	Quarter	
Natural mortality-at-age			
M_{pmax}	0.8	Quarter ⁻¹	
c_1	0.3		
M_{smax}	0.2	Quarter ⁻¹	
c_2	-0.8		
c_3	11	Quarter	
c_4 juvenile ; adult	0.03; 0.01		
Spawning habitat			
$(. s; \sigma_s)$	28; 2	°C	
α	2.0		
Adult feeding habitat			
Temperature $(. a; \sigma_a)$	22; 3	°C	
Oxygen S(half value, slope)	2; -0.1	ml .l ⁻¹	
Movement of larvae			
Diffusion	7500	Nm ² mo ⁻¹	
Advection	Mean currents in upper layer	Nm ² mo ⁻¹	
Movement of adults			
Diffusion: D_{max}	100,000	Nm ² mo ⁻¹	
Coeff.: decreasing diffusion with increasing habitat	0.04		
Advection : χ_{max}	30,000	Nm ² mo ⁻¹	
Coeff.: decreasing advection with increasing habitat	0.4		
Food ration (relative to weight of tuna)			
	0.05		

A2-2. Selectivity and length frequencies of catch

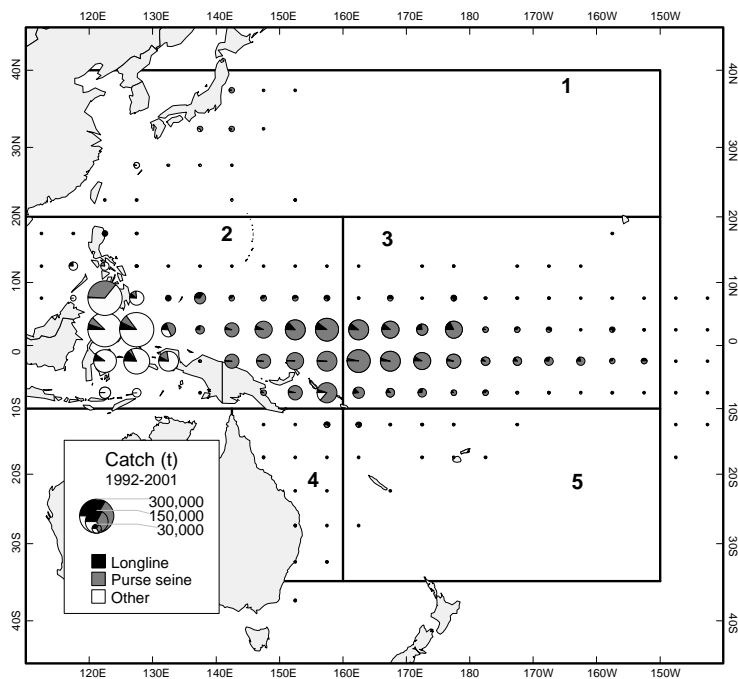


Selectivity curves of the yellowfin fisheries (by gear)

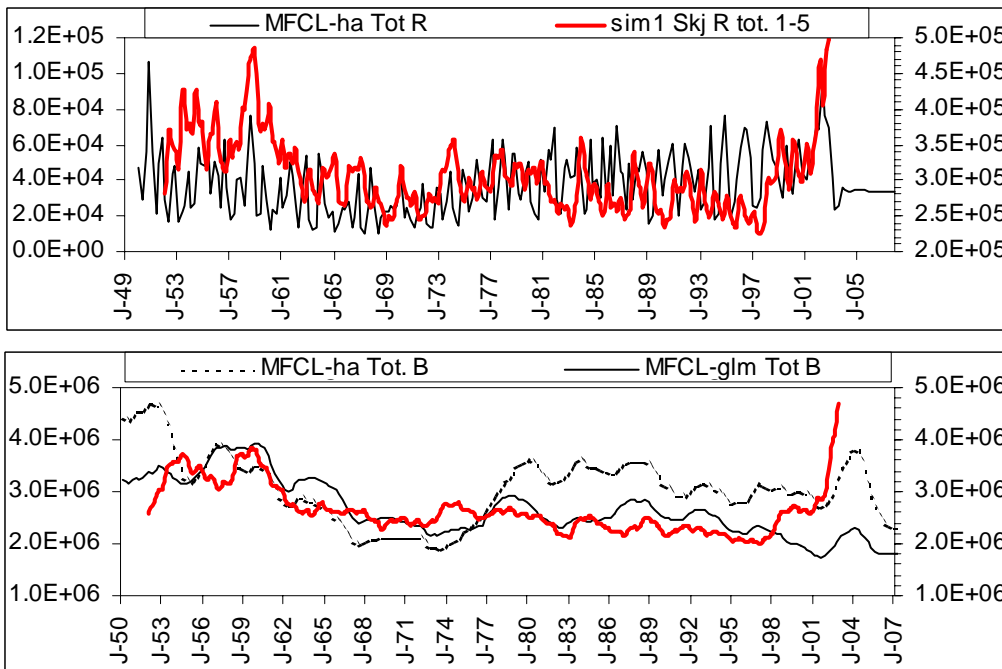


Observed (histograms) and predicted (curves) length frequencies distributions of catch by fishery (see fishery codes in Table 2)

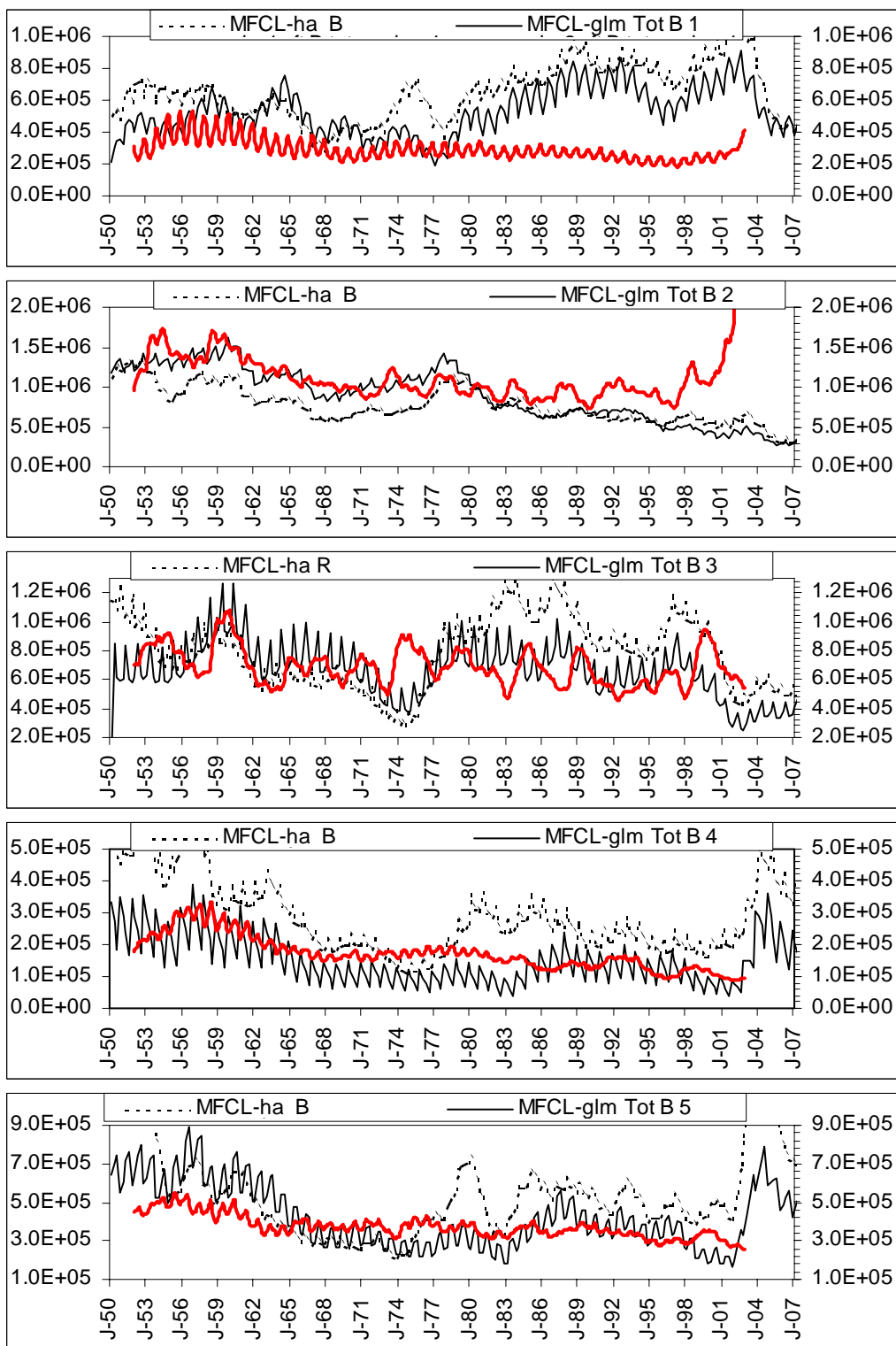
A2-3. Recruitment and biomass



Distribution of yellowfin tuna catch, 1992–2001. The heavy lines indicate the spatial stratification used in the MULTIFAN-CL model (From Hampton et al 2004).

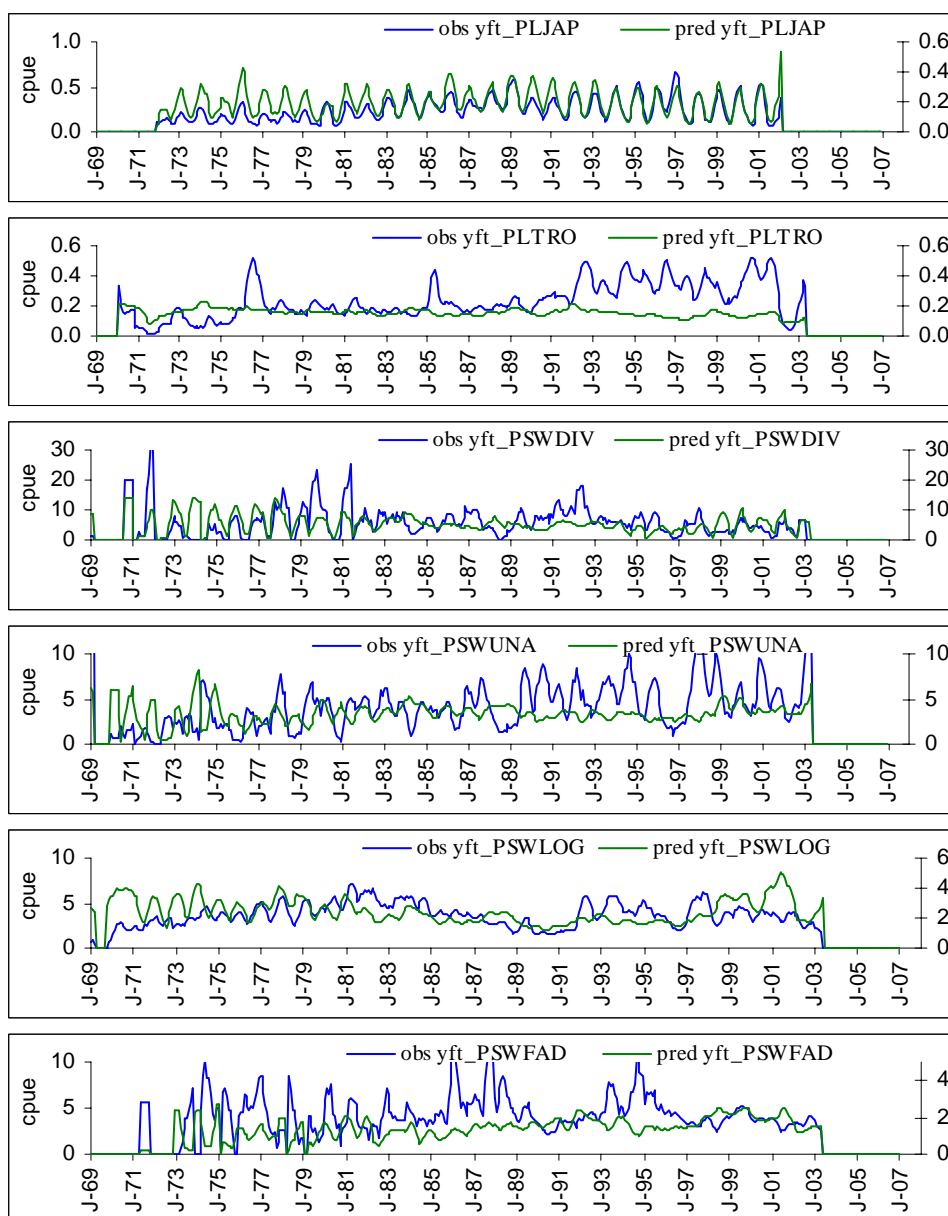


Comparison of yellowfin recruitment (top) and total biomass (tonnes) predicted in the WCPO (sum regions 1 to 5) with statistical estimates from MULTIFAN-CL (black curve)

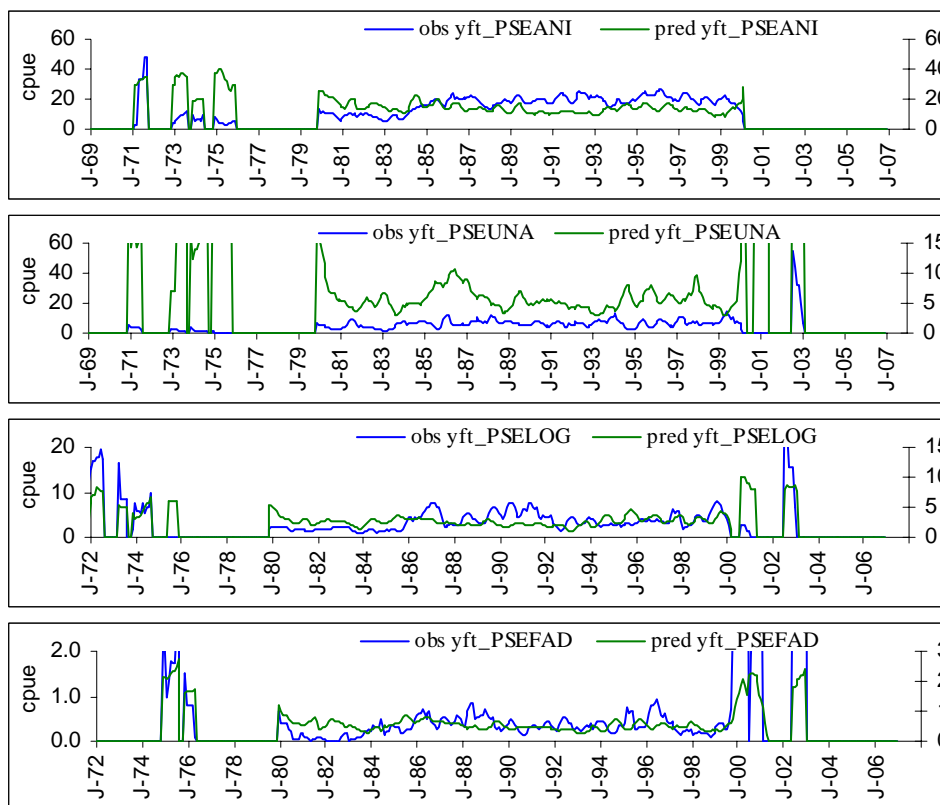


Comparison of total yellowfin biomass predicted by region 1 to 5 with statistical estimates from MULTIFAN-CL

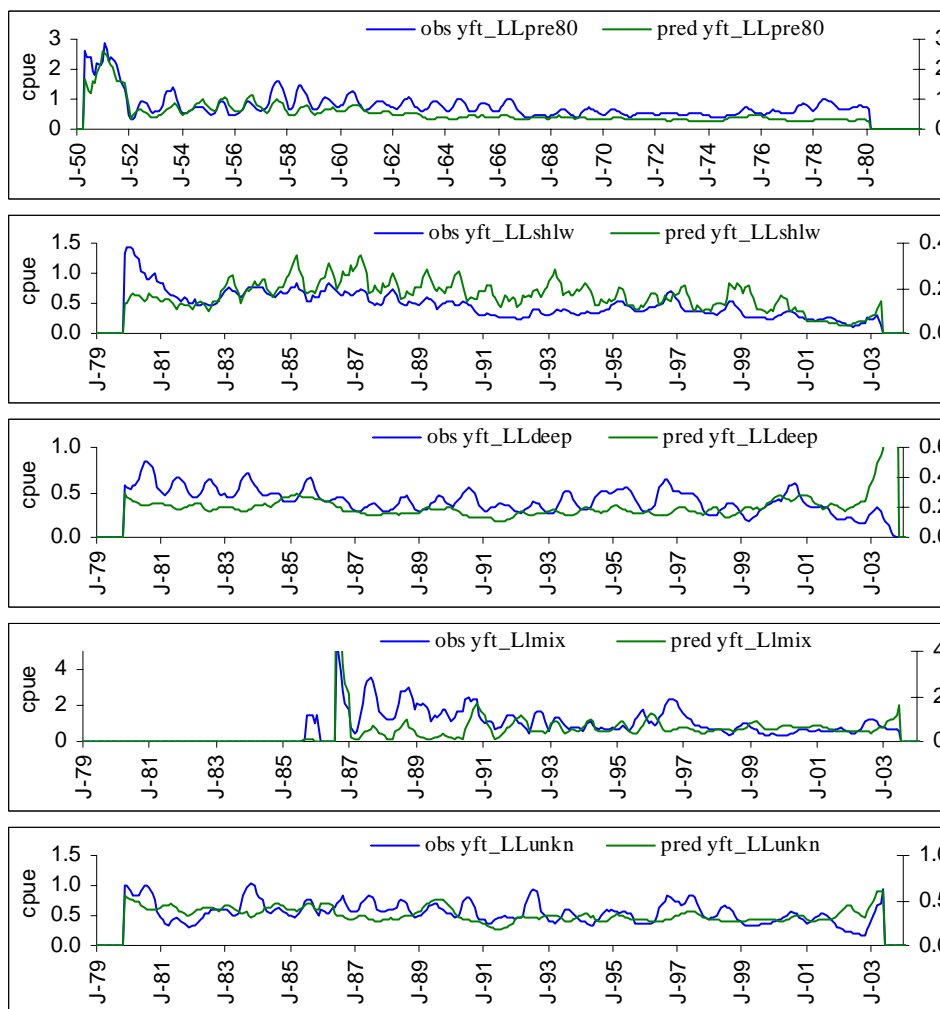
A2-4. Comparison between predicted and observed CPUE by fishery



Monthly observed and predicted skipjack CPUE by fishery in the WCPO.

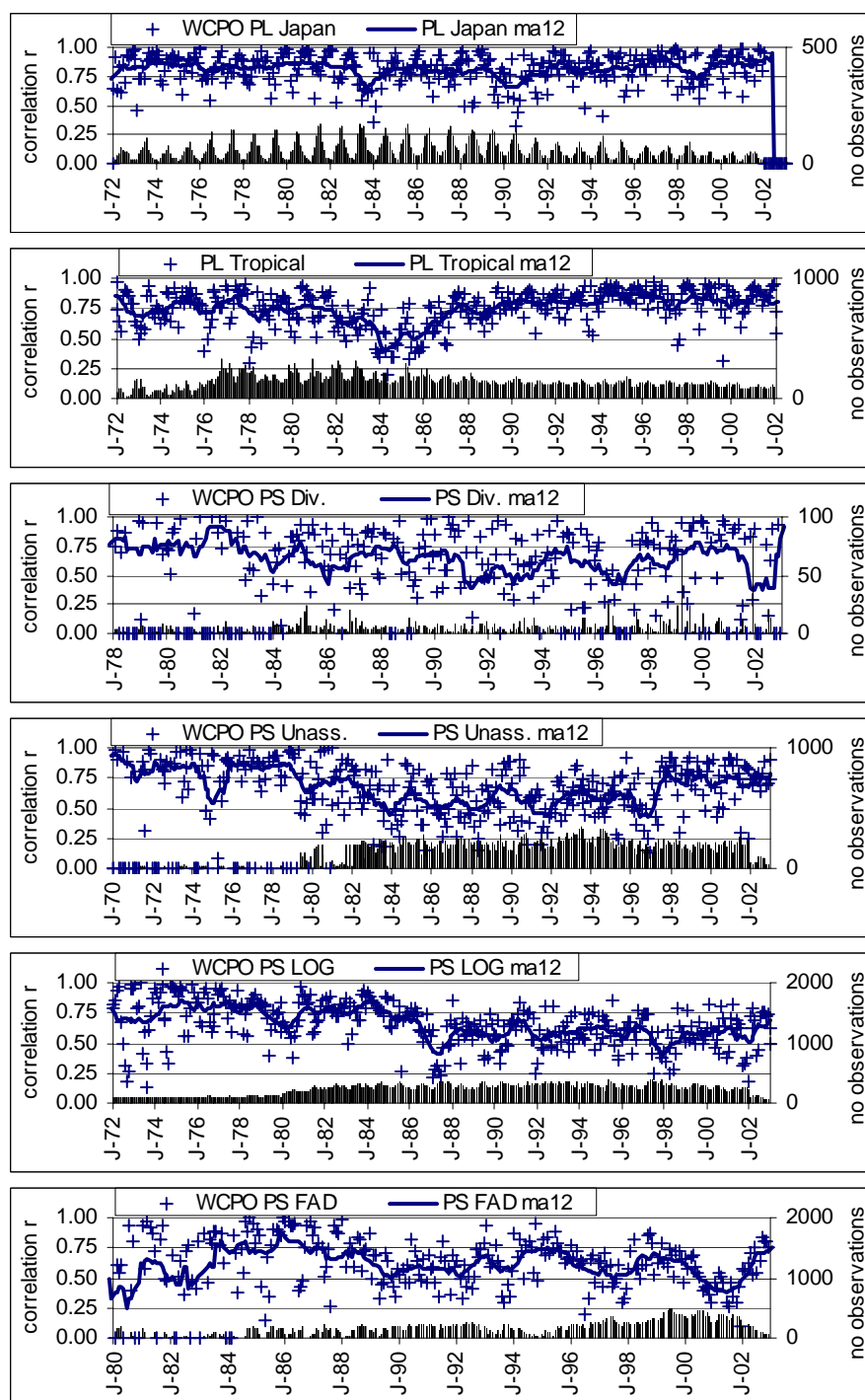


Monthly observed and predicted skipjack CPUE by fishery in theEPO

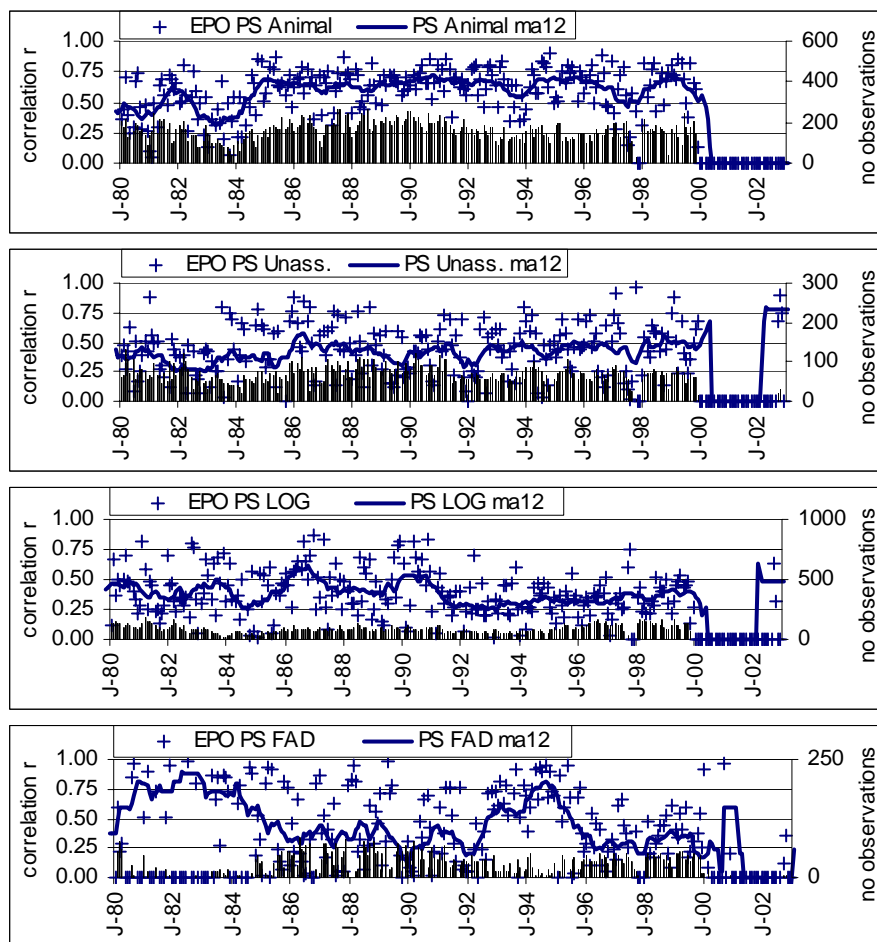


Monthly observed and predicted skipjack CPUE by longline fisheries

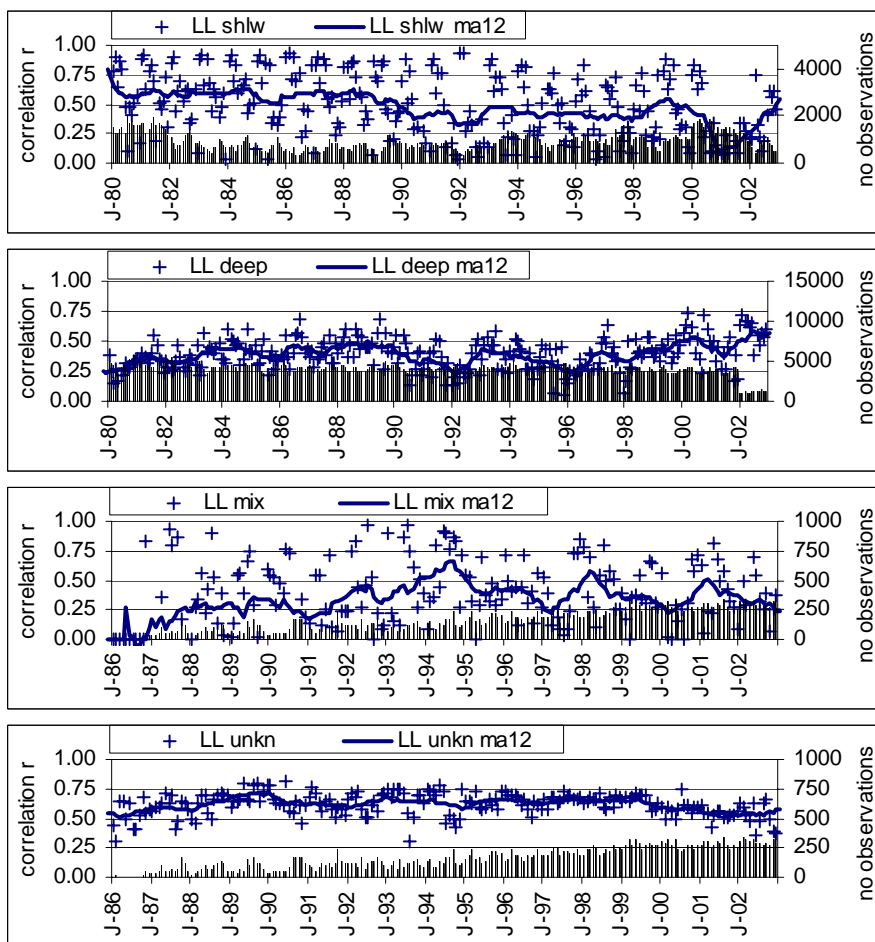
A2-5. Monthly spatial correlations between observed and predicted catch



Monthly spatial correlation by surface fishery in the WCPO. Each cross is the r -value of the monthly correlation between 1 degree square spatial predicted and observed catch, the curve is a 12 month moving average and black bars are the number of observations



Monthly spatial correlation by surface fishery in the EPO. Each cross is the r -value of the monthly correlation between 1 degree square spatial predicted and observed catch, the curve is a 12 month moving average and black bars are the number of observations



Monthly spatial correlation by longline fishery. Each cross is the r-value of the monthly correlation between 1 degree square spatial predicted and observed catch, the curve is a 12 month moving average and black bars are the number of observations